Transforming growth factor-β signaling governs the differentiation program of extravillous trophoblasts in the developing human placenta

Sandra Haider[a], Andreas Ian Lackner[b], Bianca Dietrich[a], Victoria Kunihs[a], Peter Haslinger[b], Gudrun Meinhardt[a], Theresa Maxian[a], Leila Saleh[a], Christian Fiala[c], Jürgen Pollheimer[b], Paulina A. Latos[d], and Martin Knöfler[a,1]

Abnormal placentation has been noticed in a variety of pregnancy complications such as miscarriage, early-onset preeclampsia, and fetal growth restriction. Defects in the developmental program of extravillous trophoblasts (EVTs), migrating from placental anchoring villi into the maternal decidua and its vessels, is thought to be an underlying cause. Yet, key regulatory mechanisms controlling commitment and differentiation of the invasive trophoblast lineage remain largely elusive. Herein, comparative gene expression analyses of HLA-G–purified EVTs, isolated from donor-matched placenta, decidua, and trophoblast organoids (TB-ORGs), revealed biological processes and signaling pathways governing EVT development. In particular, bioinformatics analyses and manipulations in different versatile trophoblast cell models unraveled transforming growth factor-β (TGF-β) signaling as a crucial pathway driving differentiation of placental EVTs into decidual EVTs, the latter showing enrichment of a secretory gene signature. Removal of Wingless signaling and subsequent activation of the TGF-β pathway were required for the formation of human leukocyte antigen-G$^+$ (HLA-G$^+$) EVTs in TB-ORGs that resemble in situ EVTs at the level of global gene expression. Accordingly, TGF-β–treated EVTs secreted enzymes, such as DAO and PAPPA2, which were predominantly expressed by decidual EVTs. Their genes were controlled by EVT-specific induction and genomic binding of the TGF-β downstream effector SMAD3. In summary, TGF-β signaling plays a key role in human placental development governing the differentiation program of EVTs.

human placental development | extravillous trophoblast | differentiation

Accurate control of expansion and differentiation of the human placenta is critical for a successful pregnancy. The particular organ undergoes dynamic morphological changes during gestation and fulfills multiple roles such as anchorage of the conceptus to the maternal uterus, immunological tolerance, adjustment of the maternal endocrine system, and, most important, transport of nutrients and oxygen to the developing fetus (1–5). To adapt nutritional supply throughout pregnancy, maternal blood flow to the placenta is precisely controlled. Extravillous trophoblasts (EVTs), the invasive epithelial cells of the organ, play a pivotal role in this process. EVTs develop in placental anchoring villi and migrate into the maternal decidual stroma and its vessels as so-called interstitial EVTs (iEVTs) and endovascular EVTs (eEVTs), respectively (6–8). Shortly after implantation, eEVTs plug the maternal spiral arteries, thereby preventing premature oxygen delivery to the placental villi and oxidative stress (9). However, from the 10th week of pregnancy onward, eEVTs remodel the arterioles in the decidua and first third of the adjacent myometrium in conjunction with iEVTs and maternal leukocytes (10). Thereby the spiral arteries are transformed into dilated conduits, ensuring steady low-pressure blood flow to the placenta (11). During invasion, EVTs undergo cell differentiation and acquire distinct molecular features such as a switch in integrin expression and adoption of a vascular adhesion phenotype (12, 13). Yet, EVTs also perform many other tasks during early pregnancy. They invade uterine glands, warranting early placental growth and histiotrophic nutrition of the fetus (14, 15), and infiltrate maternal lymphatics and veins, a process which is disturbed in placentae of women with recurrent pregnancy loss (16, 17). Failures in placentation and vessel remodeling have also been noticed in other pregnancy complications such as preterm labor, stillbirth, early-onset preeclampsia, and severe fetal growth restriction (18–20). Besides fetal and maternal aberrations, defects in EVT invasion, maturation, and differentiation, in situ as well as in vitro, have been observed (21–24).

Development of the EVT lineage shares many features with tumorigenesis, yet represents a highly coordinated physiological process (25, 26). In placental anchoring villi,

Significance

During pregnancy, extravillous trophoblasts (EVTs) detach from anchoring sites of the placenta, differentiate, and invade the maternal uterus to remodel its vasculature. Failures in this program contribute to placentation defects observed in gestational disorders such as spontaneous pregnancy loss, early-onset preeclampsia, and fetal growth restriction. However, critical regulators and signaling pathways controlling EVT development have been poorly elucidated. In the present study, we demonstrate that transforming growth factor-β (TGF-β) signaling plays a pivotal role in the differentiation program of EVTs. In vitro, loss of Wingless signaling was sufficient for EVT formation in self-renewing trophoblast models, whereas subsequent activation of TGF-β signaling accomplished differentiation into trophoblasts that display some features of in vivo EVTs.

multilayered EVT progenitors are formed in their proximal cell columns (CCs). Activation of canonical NOTCH1 signaling could be required for expansion of these precursors (27). In the distal part of the CC, EVT progenitors cease proliferation and undergo genome amplification (28). These herein-termed placental EVTs (pEVTs) induce characteristic marker genes, for example human leukocyte antigen-GHLA-G (29), NOTCH2 (30), ERBB2 (31), and TCF-4, a key transcription factor of canonical Wingless (WNT) signaling (25, 32). However, pEVTs subsequently differentiate into iEVTs upon detachment from anchoring villi and invasion into the decidua and further up-regulate specific proteins such as pregnancy-associated plasma protein A (PAPPA), proteoglycan 2 (PRG2), and the histamine-degrading enzyme diamine oxidase (DAO) (17, 26, 33). The two EVT populations have also been recently identified by single-cell sequencing of the fetal–maternal interface (34). Yet, our knowledge on key signaling pathways regulating differentiation of pEVTs into iEVTs remains scarce, mainly since self-renewing human trophoblast models, allowing for controllable EVT lineage formation and in vitro differentiation, have only been recently developed (35–37). Despite differences in protocols, HLA-G$^+$ EVTs were retrieved from two-dimensional (2D) trophoblast stem cells (TSCs) and 3D trophoblast organoids (TB-ORGs), developing from NOTCH1$^+$ EVT progenitors in the latter (35, 36). However, in both systems the absence of several EVT markers, such as PAPPA and DAO, has been noticed, suggesting that the in vitro generated EVTs are not fully matured (26). Hence, we hypothesized that activation of additional signaling pathways must be critical for completion of EVT differentiation. To gain novel insights into the developmental program of EVTs, we herein analyzed highly purified, donor-matched preparations of pEVTs, iEVTs, and TB-ORG–derived EVTs (TB-ORG-EVTs) using RNA sequencing (RNA-seq) and identified transforming growth factor-β (TGF-β) signaling as an activated pathway in tissue-derived EVTs. Finally, in vitro manipulation of several versatile trophoblast models confirmed the key role of TGF-β signaling in human placental EVT differentiation.

Results

Isolation and Characterization of EVTs Isolated from Placenta, Decidua, and Trophoblast Organoids.
In order to compare gene expression profiles of in situ and in vitro derived EVT populations,

HLA-G$^+$ EVTs were purified from first-trimester placenta, decidua, and TB-ORGs of the same patient ($n = 3$). While pEVTs and iEVTs were directly prepared from placental and decidua basalis tissues, respectively, purified placental cytotrophoblasts (CTBs) were used for establishing self-renewing TB-ORGs in the presence of epidermal growth factor (EGF), the WNT activator CHIR99021, and the TGF-β receptor (ALK4/5/7) inhibitor A8301 as described (35, 38). TB-ORG-EVTs were generated by withdrawing CHIR99021 from these cultures (WNT$^-$ condition) (Fig. 1A). All EVT populations expressed HLA-G, which was utilized for immunopurification (Fig. 1B). To assess purity, HLA-G$^+$ EVTs as well as remaining cells were tested for specific markers of CTB, EVT, and stromal cell populations (*SI Appendix*, Fig. S1). In contrast to CTBs, pEVTs and iEVTs expressed EVT-specific proteins such as HLA-G (29), fibronectin 1 (FN1) (39), and PRG2 (17) but lacked markers of decidual stromal cells such as the Thy-1 cell-surface antigen (THY1) (40), aminopeptidase N (CD13) (41), Dickkopf-1 (DKK1) (42), and insulin-like growth factor–binding protein 1 (IGFBP-1) (43) (*SI Appendix*, Fig. S1A). Flow cytometry data revealed that immunopurification had yielded EVT populations with a high degree of purity (*SI Appendix*, Fig. S1 *B* and *C*).

EVTs, Purified from First-Trimester Placenta, Decidua, and Organoids, Express Specific Gene Signatures.
To delineate possible differences between EVT subtypes, immunopurified HLA-G$^+$ cells were subjected to RNA-seq, bioinformatics, and gene expression analyses (Fig. 2). Raw RNA-seq data of pEVTs, iEVTs, and TB-ORG-EVTs are accessible at the Gene Expression Omnibus (GEO) database (accession no. GSE188352). Principal-component analysis (PCA) (Fig. 2A) and hierarchical clustering (*SI Appendix*, Fig. S2A) revealed strong similarities among pEVT, iEVT, and TB-ORG-EVT cell preparations, respectively; 7,211 transcripts were common to all EVT cell types, whereas pEVT, iEVT, and TB-ORG-EVTs uniquely expressed 195, 831, and 266 genes, respectively (Fig. 2B). Expression of the established pEVT markers *ERBB2* (31), *WWTR1*, encoding TAZ (38), *NOTCH2* (30), *ITGA5* and *ITGB1* (12), *CDKN1C* (28), *CBLB* (44), and *TCF7L2* (32) was detected in TB-ORG-EVTs as well as at a lower level in iEVTs (*SI Appendix*, Fig. S2B). *SPINT1/*HAI-1, a marker for proliferative CTBs and CC trophoblasts, and *CDH5/*VE-cadherin, localizing to a subset
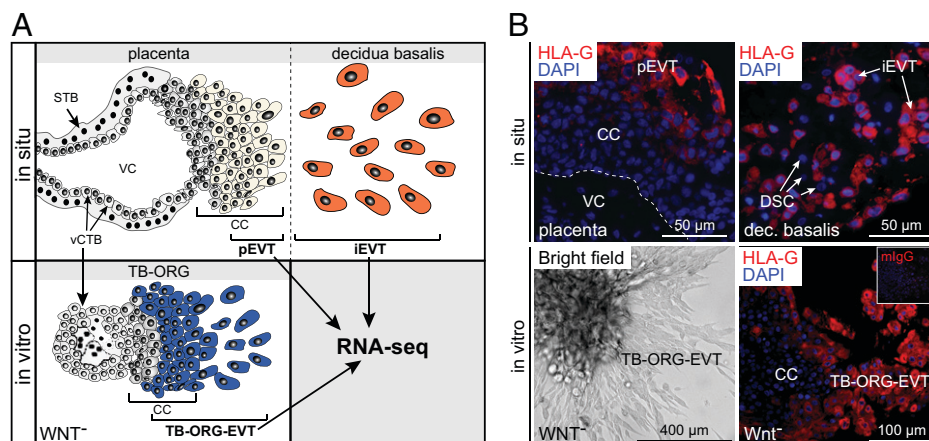
Fig. 1. Localization and identification of different EVT cell types used for bulk RNA-seq. (*A*) Schematic depiction showing localization of pEVTs, decidual iEVTs, and TB-ORG-EVTs during early pregnancy. Whereas pEVTs and TB-ORG-EVTs develop from proliferative CC trophoblasts, iEVTs detach from CCs at anchoring sites and migrate into the maternal decidua. TB-ORG-EVTs were generated in vitro by removing the GSK-3β inhibitor/canonical WNT activator CHIR22901 from the stem cell medium for 8 d (WNT$^-$ condition). STB, syncytiotrophoblast; VC, villous core; vCTB, villous cytotrophoblast. (*B*) Representative immunofluorescence images (eighth week of pregnancy) showing HLA-G expression in placental anchoring villi, decidua basalis, and Wnt$^-$ TB-ORGs of the same patient. HLA-G$^-$ decidual stromal cells (DSCs) are marked. Nuclei are visualized by DAPI staining. Mouse immunoglobulin G (mIgG) isotype antibodies were used as negative control.
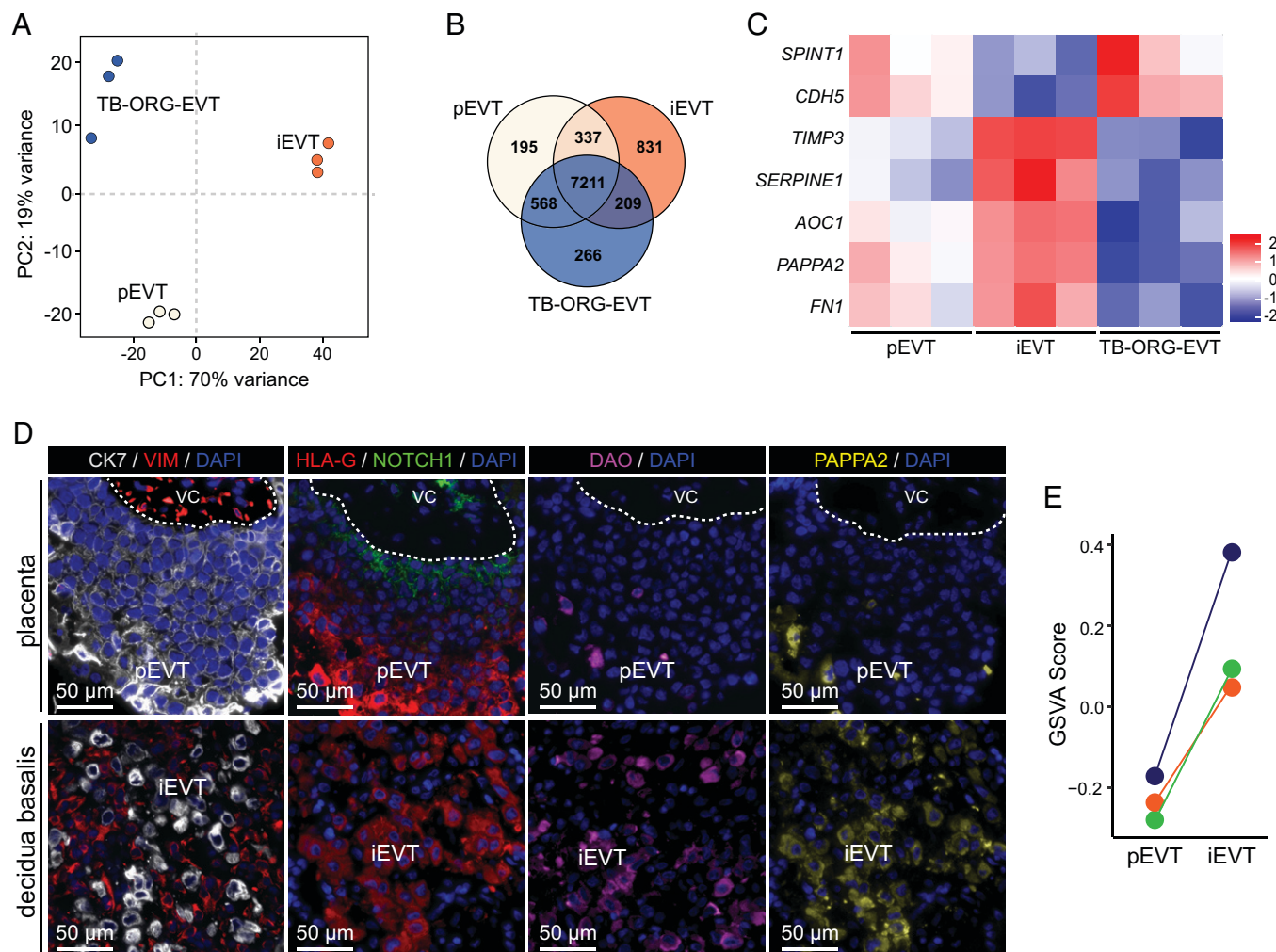
Fig. 2. Expression analyses of pEVTs, iEVTs, and TB-ORG-EVTs. Placenta and decidua basalis tissues (*n* = 3; one sample from the seventh week and two samples from the eighth week of pregnancy) were used for preparation of donor-matched pEVTs, iEVTs, and TB-ORG-EVTs. Transcript expression was analyzed by bulk RNA-seq. (*A*) PCA demonstrating donor-independent clustering of the three pEVT, iEVT, and TB-ORG-EVT mRNA samples, respectively. (*B*) Venn diagram illustrating numbers of common and uniquely expressed genes in pEVTs, iEVTs, and TB-ORG-EVTs. (*C*) Heatmap showing expression of selected EVT markers. (*D*) Immunofluorescence of EVTs in serial sections of first-trimester placenta (CC) and decidua of the same patient. Representative images (eighth-week pregnancy tissues) are shown. Sections were counterstained with DAPI. CK7, cytokeratin 7; VIM, vimentin. (*E*) GSVA of a hand-curated secretory gene signature in pEVTs and iEVTs. Colors refer to pEVT and iEVT scores of the three different patients.

of pEVTs adjacent to the proximal CC (27), also decreased in iEVTs compared with pEVTs and/or TB-ORG-EVTs (Fig. 2*C* and *SI Appendix,* Fig. S2 *C–E*). In contrast, transcript and/or protein levels of EVT-secreted factors, for example *TIMP3* (45), *SERPINE1* (46), *AOC1*/DAO (33), PAPPA2 (47), and FN1 (39), were elevated in iEVTs (Fig. 2*C* and *SI Appendix,* Fig. S2 *C and D*). DAO was detected in 5 to 8% of pEVTs, largely colocalizing with PAPPA2, whereas 55 to 65% and 70 to 80% of iEVTs were positive for DAO and PAPPA2, respectively (Fig. 2*D*). Both DAO and PAPPA2 were absent from TB-ORG-EVTs (Fig. 2*C* and *SI Appendix,* Fig. S2*E*). Furthermore, gene set variation analysis (GSVA) using a secretome-specific gene signature indicated higher GSVA scores in iEVTs compared with pEVTs (Fig. 2*E*). Accordingly, numerous transcripts encoding secreted proteins were elevated in iEVTs such as proteases (*MMP11, HTRA1, PAPPA, PAPPA2, CTSB*), protease inhibitors (*TIMP2, TIMP3, SERPINE1, SERPINE2, SERPING1*), glycoproteins (*CSH1, EBI3, FBLN1*), and regulators of angiogenesis/vessel function (*ISM2, FLT1, ADM, GRN*) (*SI Appendix,* Fig. S2*F*). In summary, gene expression analyses suggested that, in comparison with in situ EVTs, TB-ORG-EVTs were less matured.

Differentiation of EVTs Is Associated with TGF-β Signaling. Next, we next sought to unravel pathways critically involved in EVT maturation. Gene set enrichment analysis revealed that different biological processes including angiogenesis, the reactive oxygen species pathway, and signaling through TGF-β and STAT3 were significantly up-regulated in iEVTs compared with pEVTs, while MYC target genes were down-regulated (*SI Appendix,* Fig. S3*A*). Not surprisingly, TGF-β signaling was also up-regulated in pEVTs compared with the A8301-treated TB-ORG-EVTs, while STAT3 and canonical WNT signaling showed positive trends (*SI Appendix,* Fig. S3*B*). Furthermore, differentiation of pEVTs into iEVTs was associated with increased messenger RNA (mRNA) expression of canonical TGF-β targets such as *FN1, TIMP3, NOTUM, PAPPA2,* and *CTGF* (*SI Appendix,* Fig. S3 *C and D*) and with elevated transcript levels of TGF-β receptor 1 (*TGFBR1*, encoding ALK5) and *TGFBR2* (*SI Appendix,* Fig. S3 *E and F*). In agreement, TGFβR1 and TGFβR2 were hardly detectable in first-trimester placenta in situ, whereas iEVTs of the decidua showed stronger signals (*SI Appendix,* Fig. S3*G*). The downstream effector *SMAD3* was highly expressed in iEVTs but absent from proliferative CTBs (*SI Appendix,* Fig. S3*F*). In summary, bioinformatics and

expression analyses suggest that TGF-β signaling could play a major role in the developmental program of EVTs.

Activation of TGF-β Signaling Governs EVT Differentiation. To investigate the role of TGF-β signaling in EVT differentiation, HLA-G⁺ EVTs were isolated from WNT⁻ (removal of CHIR99021) TB-ORGs in the presence of the TGF-β signaling inhibitor A8301 (condition DIFF-1), as well as from WNT⁻ TB-ORGs cultured in the absence of A8301 (condition DIFF-2), allowing for autocrine activation of the pathway (Fig. 3A and *SI Appendix*, Fig. S4A). To further increase TGF-β signaling, recombinant TGF-β1 was added to WNT⁻ A8301⁻ TB-ORGs (condition DIFF-3). Sequential withdrawal of CHIR99021 and A8301 was critical for EVT formation in TB-ORGs, whereas simultaneous removal of the inhibitors (condition DIFF-4 and DIFF-5) blocked outgrowth and differentiation (*SI Appendix*, Fig. S4 *A and B*). While condition DIFF-1 was sufficient for the expression of HLA-G, VE-cadherin, and TAZ, activation of

TGF-β signaling (DIFF-2) was required for the induction of FN1, DAO, and PAPPA2 (Fig. 3 *B and C*). The latter were further up-regulated upon supplementation with TGF-β1 (DIFF-3), while VE-cadherin decreased. Like in anchoring villi (Fig. 2D), DAO localized to a small subset of distal CC EVTs in TGF-β1–stimulated TB-ORGs (Fig. 3C). Similar to TB-ORGs, DIFF-1 provoked HLA-G expression in 2D TSC lines, while activation of TGF-β signaling (DIFF-2 and DIFF-3) was necessary for the expression and secretion of FN1, DAO, and PAPPA2 (Fig. 3 *D and E*).

TGF-β-SMAD3 Signaling Promotes Expression of iEVT-Specific Genes. Next, signaling of TGF-β through its downstream effector SMAD3 was analyzed in first-trimester villous explant cultures, primary EVTs, TSCs, and TB-ORGs (Fig. 4 and *SI Appendix*, Fig. S4). CC outgrowth and HLA-G expression were not affected by A8301 in villous explants (Fig. 4 *A and B* and *SI Appendix*, Fig. S4C). However, the inhibitor increased
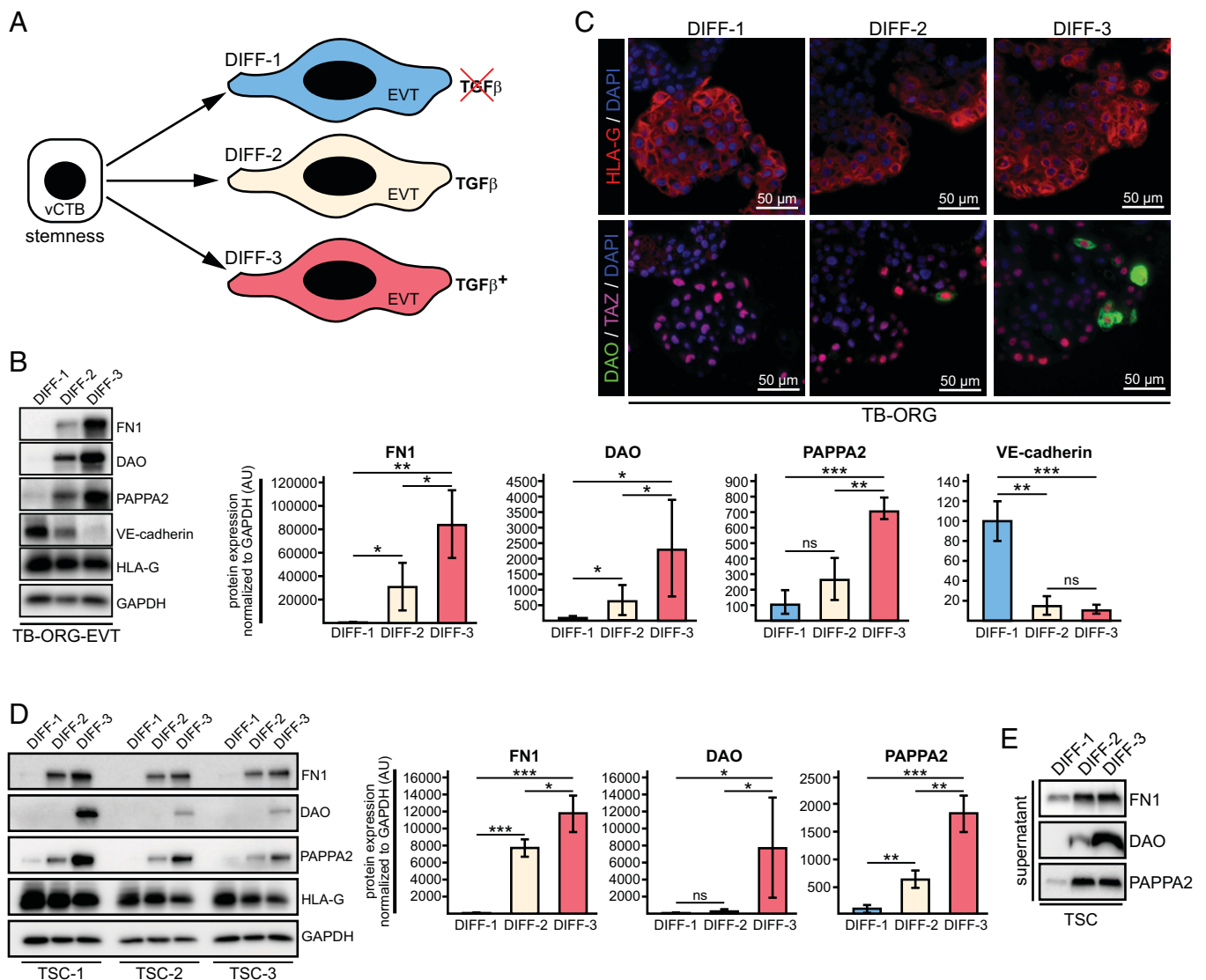
Fig. 3. TGF-β signaling governs EVT differentiation. (A) Schematic depiction of culture conditions used for EVT differentiation in 3D TB-ORGs and 2D TSC lines (DIFF-1 to -3). After 10 d of cultivation in the different media, HLA-G⁺ EVTs and tissue sections were prepared from TB-ORGs, whereas whole-protein lysates were prepared from cells and supernatants of TSCs. (B and D) Representative Western blots (*Left*) and quantifications (*Right*) of EVT markers in TB-ORG-EVTs (B) or TSCs (D) after cultivation in DIFF-1 (WNT⁻ A8301⁺), DIFF-2 (WNT⁻ A8301⁻), or DIFF-3 (WNT⁻ A8301⁻/TGF-β1⁺) are shown. Signals were normalized to GAPDH, used as loading control. Condition DIFF-1 was arbitrarily set to 100%. Bar graphs in B and D show mean values ± SD derived from four TB-ORG cultures (sixth to seventh week) and three TSC lines (sixth to seventh week). *P < 0.05, **P < 0.01, ***P < 0.001; ns, not significant. AU, arbitrary units. (C) Immunofluorescence showing localization of HLA-G, TAZ, and DAO in tissue sections of differentiating TB-ORGs. (E) Representative Western blot depicting soluble FN1, DAO, and PAPPA2 levels, normalized to cellular protein concentration, in supernatants (day 10) of TSCs.
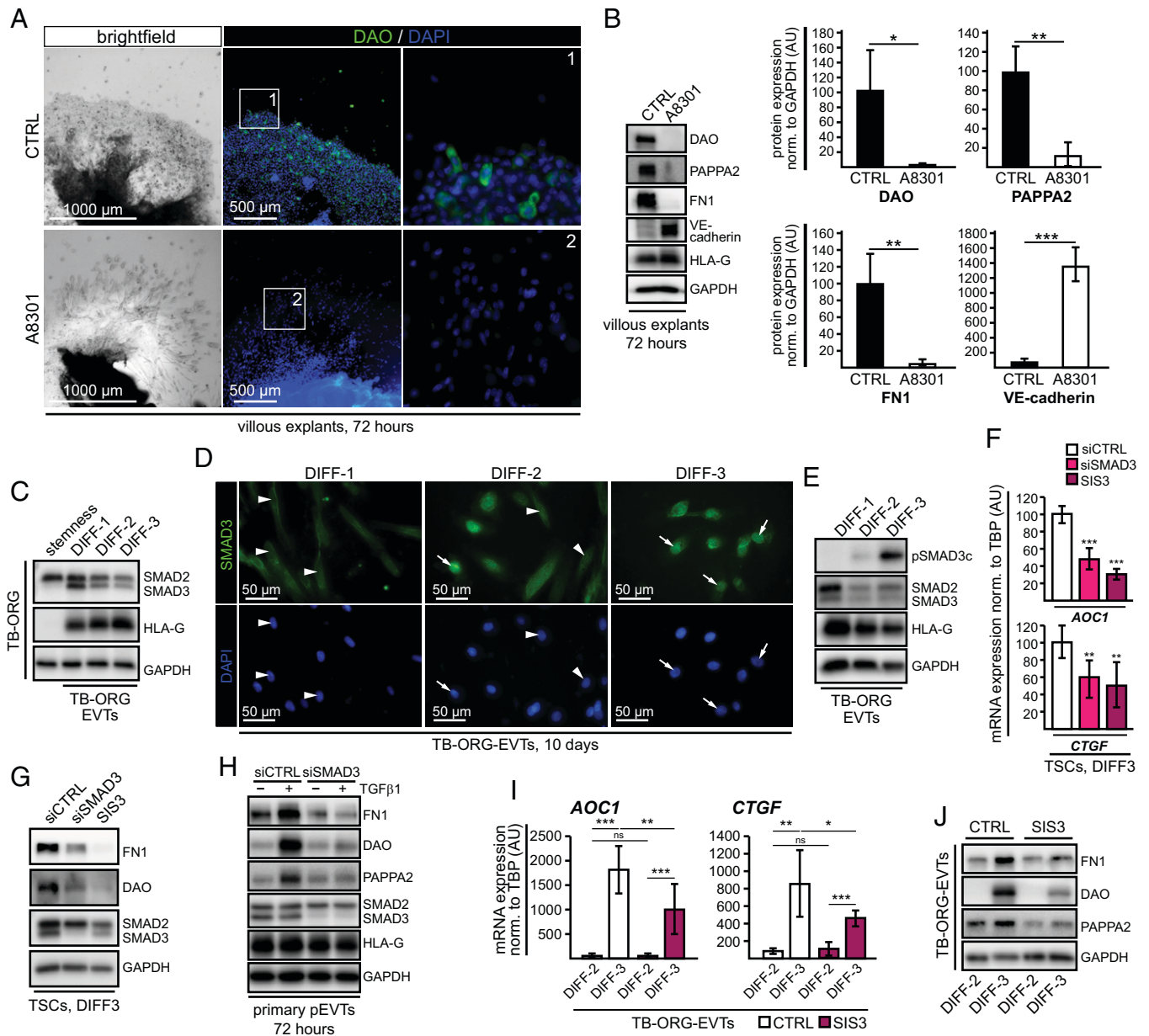
Fig. 4. TGF-β–mediated EVT differentiation requires SMAD3 activation. (*A*) Representative images showing outgrowth (bright-field) and DAO expression (immunofluorescence, whole-mount staining) in villous explant cultures (eighth-week placenta) seeded onto collagen I in the absence (control; CTRL) or presence of A8301. Nuclei are stained with DAPI. (*A, Right*) Magnification of *Insets* 1 and 2. (*B*) Western blot (*Left*) and quantification (*Right*) showing EVT marker expression in untreated (CTRL) and A8301-treated villous explant-derived EVTs. Bar graphs depict mean values ± SD obtained from four different cultures (sixth- to eighth-week placentae) normalized to GAPDH. CTRL was set to 100%. (*C* and *E*) Representative Western blots showing SMAD2/3 (*C*) and pSMAD3C (*E*) protein expression in HLA-G–purified EVTs of TB-ORGs (sixth week). The latter were cultivated under condition DIFF-1 (A8301+), DIFF-2 (A8301−), or DIFF-3 (A8301−/TGF-β1+) as depicted in Fig. 3*A* and *SI Appendix*, Fig. S4*A*. GAPDH was used as loading control. (*D*) Immunofluorescence images showing SMAD3 localization in TB-ORG-EVTs (sixth week). SMAD3+ (arrows) and SMAD3− nuclei (arrowheads) are shown. Nuclei are stained with DAPI. (*F* and *G*) qPCR (*F*) (n = 3; mean values ± SD) and immunoblot (*G*) showing down-regulation of EVT markers in differentiated TSCs (condition DIFF-3) treated with nontargeting control (siCTRL, set at 100%), SMAD3 siRNAs (siSMAD3), or the SMAD3-specific inhibitor SIS3. Transcript levels, measured in duplicates, were normalized to *TBP*. Mean values ± SD of three different TSC preparations (sixth to seventh week) are depicted. (*H*) Representative Western blot illustrating TGF-β1– and SMAD3-dependent expression of EVT markers in primary pEVTs after incubation with siSMAD3. (*I* and *J*) qPCR (*I*) (n = 3; mean values ± SD) and Western blot (*J*) showing reduced iEVT marker expression in TB-ORG-EVTs (sixth week) after TGF-β activation (conditions DIFF-2 and DIFF-3) and treatment with SIS3. GAPDH was used as loading control. *P < 0.05, **P < 0.01, ***P < 0.001; ns, not significant.

CDH5/VE-cadherin and repressed *CTGF*, *AOC1*/DAO, FN1, and PAPPA2 in these cultures, whereas active TGF-β signaling had the opposite effect (Fig. 4 *A* and *B* and *SI Appendix*, Fig. S4 *C* and *D*). In analogy, TGF-β signaling also elevated *AOC1*/DAO, FN1, PAPPA2, and *TIMP3* in cells and supernatants of HLA-G–purified pEVTs cultivated on fibronectin (*SI Appendix*, Fig. S4 *E–G*). In vivo, SMAD3 was detectable in nuclei of iEVTs and in a subset of pEVTs, located in the outermost regions of the distal CC (*SI Appendix*, Fig. S4*H*). Whereas

condition DIFF-1 was sufficient for SMAD3 expression in TB-ORG-EVTs (Fig. 4*C*), activation of TGF-β signaling was required for SMAD3 nuclear recruitment and its canonical, C-terminal phosphorylation (pSMAD3C) (Fig. 4 *D* and *E*). Accordingly, inhibition of the signaling pathway decreased numbers of SMAD3+ nuclei in primary pEVTs and abolished nuclear pSMAD3C in these cells (*SI Appendix*, Fig. S4 *I* and *J*). TGF-β inhibition also eliminated coexpression of SMAD3 and DAO in EVTs of villous explant cultures (*SI Appendix*,

Fig. S4K). Gene silencing of *TGFBR1*, *TGFBR2*, or both receptors decreased *AOC1*/DAO as well as *CTGF* and FN1 expression in primary pEVTs and TSCs (*SI Appendix*, Fig. S4 *L–O*). Moreover, small interfering RNA (siRNA)–mediated down-regulation of SMAD3 diminished *AOC1*/DAO, *CTGF*, and FN1 expression in TSCs, cultivated under condition DIFF-3 (Fig. 4 *F* and *G*), and abrogated TGF-β1–dependent expression of FN1, DAO, and PAPPA2 in primary pEVTs (Fig. 4*H*). Likewise, transcript and protein levels of these iEVT markers declined in differentiating TSCs and TB-ORGs upon treatment with the selective SMAD3 inhibitor SIS3 (48) (Fig. 4 *F*, *G*, *I*, and *J*).

Furthermore, genomic sequences of *AOC1*, *PAPPA2*, *FN1*, and *CTFG*, previously identified as SMAD3-binding regions, were retrieved from the Gene Transcription Regulation Database or selected publications (*SI Appendix*, Fig. S5*A*). Primers were designed for these sites (*SI Appendix*, Table S2) and used for qPCR after SMAD3-specifc chromatin immunoprecipitation with chromatin isolated from primary CTBs or HLA-G–purified EVTs. Increased binding of SMAD3 to the *AOC1* promoter and an upstream enhancer region was identified in EVTs, whereas a distal enhancer of the *PAPPA2* gene was recognized (*SI Appendix*,

Fig. S5*B*). Moreover, interaction of SMAD3 with proximal and distal genomic regions of *FN1* and *CTGF*, respectively, was detected in these cells (*SI Appendix*, Fig. S5*B*). In conclusion, activation of TGF-β-SMAD3 seemed to be crucial for EVT differentiation and iEVT-specific gene expression.

TGF-β Signaling Impairs Extravillous Trophoblast Motility. Inspection of the different trophoblast models revealed that TGF-β inhibition altered cellular appearance as well as migratory behavior of EVTs (Fig. 5). In contrast to the epithelial phenotype of controls, EVTs of A8301-treated villous explants, TB-ORGs, and 2D primary cultures displayed a spindle-shaped, fibroblast-like morphology (Fig. 5 *A* and *B* and *SI Appendix*, Fig. S6*A*). TGF-β inhibition in primary pEVTs promoted lamellipodium and actin stress fiber formation indicative of directed cell movement (49), whereas control cultures presented a dense crisscross F-actin/α-actinin meshwork (*SI Appendix*, Fig. S5*B*). Proteins associated with focal adhesions (vinculin, paxillin, zyxin) were observed at the leading edge of A8301-treated primary pEVTs and TB-ORG-EVTs, whereas a radial distribution was detected in cells with activated TGF-β
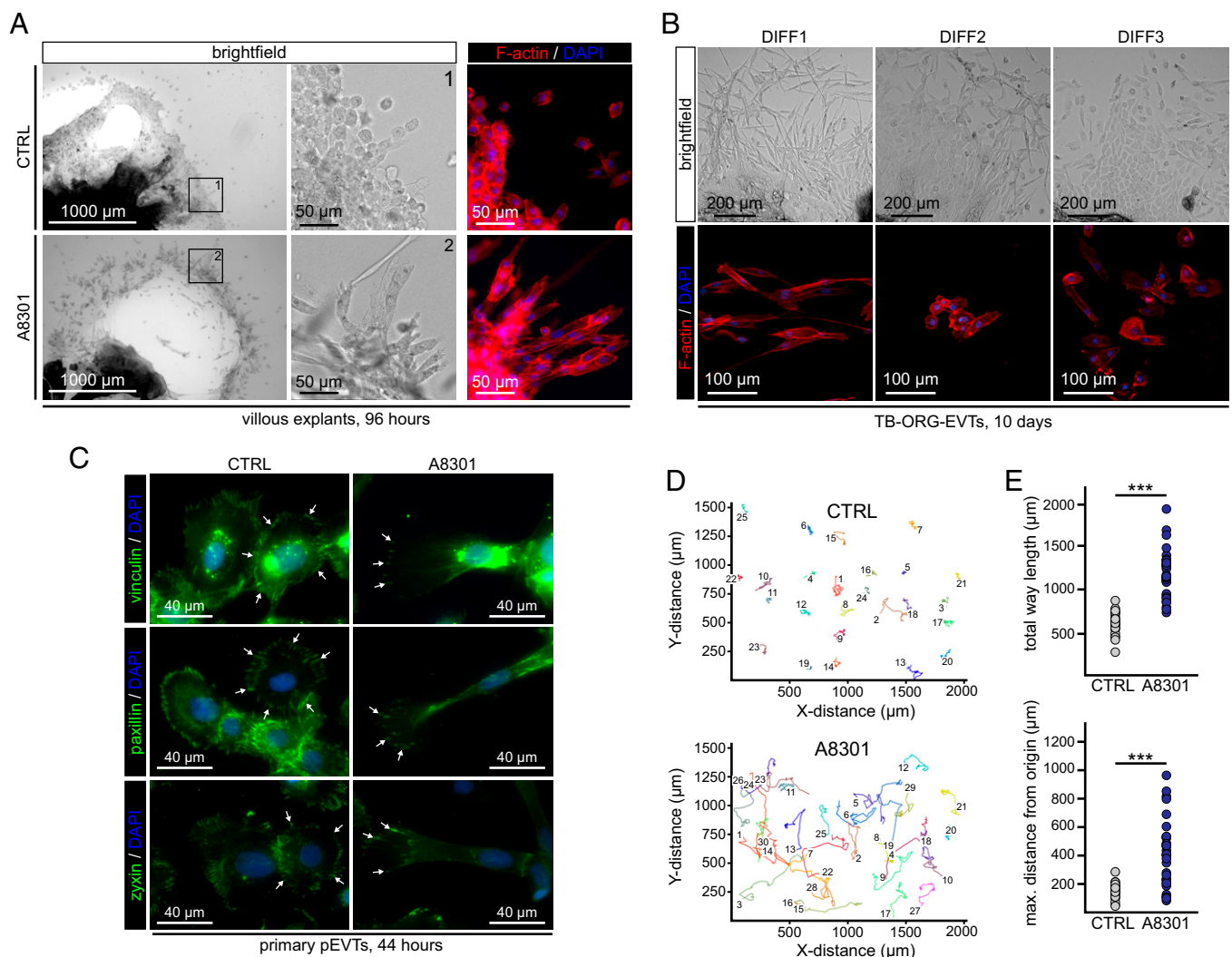
Fig. 5. Inhibition of TGF-β signaling increases EVT motility and promotes lamellipodium formation. F-actin was visualized by fluorescence-labeled phalloidin staining. Nuclei were stained with DAPI. (*A*) Villous explants (seventh week) cultivated in the absence (CTRL) or presence of A8301. (*A*, *Middle* and *Right*) Magnification of *Insets* 1 and 2 showing selected areas with EVTs. (*B*) Morphology of EVTs in TB-ORGs (sixth week) cultured under different conditions (DIFF-1 to -3, indicated in Fig. 3*A*). (*C*) Immunofluorescence showing proteins associated with focal adhesions in untreated (CTRL) and A8301-treated HLA-G–purified primary EVTs (eighth week) cultured on fibronectin (*Arrows* depict focal adhesions). (*D*) Cell tracking of 25 (CTRL) and 30 (A8301-treated) primary pEVTs migrating on fibronectin for 67 h. (*E*) Quantification of EVT motility based on migration distances of individual cells shown in *D*. Total-way length (*Upper*) and maximal distance from origin (*Lower*) are shown. ***$P < 0.001$.

signaling (Fig. 5C and *SI Appendix*, Fig. S6C). Accordingly, inhibition of TGF-β signaling increased motility of pEVTs on fibronectin (Fig. 5 D and E and Movies S1 and S2), as well as migration through fibronectin-coated transwells (*SI Appendix*, Fig. S6D). In summary, autocrine TGF-β signaling suppressed the mesenchymal phenotype of EVTs and impaired their migration.

TGF-β–Activated TB-ORG-EVTs Resemble Tissue-Derived EVTs.
To investigate global effects of TGF-β signaling on EVTs, TB-ORGs, isolated from three different first-trimester placentae (sixth to eighth week), were treated with the different conditions described in Fig. 3A. HLA-G⁺ EVTs were purified from these cultures and subjected to RNA-seq (raw data are available at the GEO; accession no. GSE188352) and bioinformatics analyses were conducted in comparison with the donor-matched EVT samples (Fig. 6). PCA and hierarchical clustering revealed that EVTs isolated from condition DIFF-2 (A8301⁻) or DIFF-3 (A8301⁻, TGF-β1⁺) display similarities with in situ pEVTs at the level of global mRNA expression (Fig. 6 A and B). TGF-β–activated TB-ORG-EVTs up-regulated transcripts that were elevated in pEVTs and iEVTs encoding secreted enzymes (*PAPPA, PAPPA2, AOC1, HTRA1*), canonical *TGF-β* targets (*NOTUM, CTGF, FN1*), and angiogenic factors (*ISM2, FLT1, GRN*) (*SI Appendix*, Fig. S7). Others that were enriched in iEVTs vs. pEVTs (e.g., *CTSB, TIMP2, ADM, FOS, JUN, TGFBR1*) were not increased by the TGF-β1 treatment (*SI Appendix*, Fig. S7). Interestingly, some mRNAs that were abundant in pEVTs and TB-ORG-EVTs and expressed at lower levels in iEVTs also declined upon TGF-β1 activation, for example the distal CC markers *TCF7L2* and *NOTCH2* and components of the WNT pathway (*FZD5, FZD6, LRP5,*

WNT7A) (*SI Appendix*, Fig. S7). Compared with DIFF-1 (A8301⁺), DIFF-2 and DIFF-3 reduced the number of differentially expressed genes between TB-ORG-EVTs and pEVTs or iEVTs, respectively (Fig. 6C). In conclusion, activation of TGF-β signaling in TB-ORG-EVTs recapitulates major aspects of in situ EVTs.

Discussion

Factors and signaling cascades controlling trophoblast invasion and migration have been widely studied (25, 50). However, key mechanisms governing EVT progenitor development and differentiation have only recently begun to emerge. While expansion and survival of proliferative, ITGA2⁺ EVT progenitors could be controlled by NOTCH1 (27, 51), EVT differentiation was shown to be associated with the activation of specific pathways such as hypoxia-inducible factor–mediated signaling and canonical WNT signaling (32, 35, 52). Low oxygen triggers NOTCH1 expression in EVT progenitors, an early step of EVT lineage development, and promotes differentiation of TSCs and primary CTBs involving downstream targets such as ASCL2 (27, 52, 53). The role of canonical WNT signaling in placentation seems to be complex. Whereas activation of WNT by CHIR99021 is necessary for trophoblast stemness, loss of WNT is required for the formation of CC/NOTCH1⁺ EVT progenitors (35). Differentiation of these precursors into pEVTs is achieved by autocrine reactivation of the pathway, accompanied by the induction of the critical WNT downstream effector TCF-4 that also controls EVT migration (32, 35).

Yet despite the identification of several regulatory mechanisms, a deeper understanding of EVT differentiation, and in particular how decidual iEVTs develop, is lacking. On the one hand, the availability of early-pregnancy tissues for isolating pEVTs and iEVTs is limited. On the other hand, the traditional culture conditions for 2D primary CTBs, spontaneously differentiating in vitro, did not allow investigating EVT formation in a controllable manner. Recently, however, first protocols for initiation and differentiation of EVTs were established using self-renewing 2D TSCs and 3D TB-ORGs (35, 36). Removal of CHIR99021 and the presence of the TGF-β inhibitor A8301 and Matrigel were sufficient to generate HLA-G⁺ EVTs in both systems. TSCs were additionally treated with neuregulin-1 and increased concentrations of A8301 for EVT differentiation (36). While inactivation of TGF-β signaling was shown to be critical for the induction of human trophectodermal stem cells from naive pluripotent stem cells and for the expansion of postimplantation TSCs and TB-ORGs (35–37, 54, 55), continuous inhibition of the pathway during EVT differentiation remained questionable to us. The absence of EVT markers such as DAO and PAPPA (25, 26), as well as the spindle-shaped morphology of EVTs in the presence of A8301 (36) (Fig. 5), contrasting the appearance of in situ EVTs, prompted us to reinforce the culture conditions, particularly by activating TGF-β signaling at a later stage of EVT differentiation. Indeed, both EVTs and decidua are rich sources of TGF-β ligands (56, 57), suggesting that particular cytokines could play crucial roles in EVT differentiation.

We decided to perform RNA-seq and bioinformatics analyses of EVTs generated in TB-ORGs. In analogy to the in vivo situation, TB-ORG-EVTs develop in 3D from NOTCH1⁺ CC progenitors (27, 35), whereas the path of differentiation has not been defined in 2D cultured TSCs. In addition, TGF-β–activated TB-ORG-EVTs were compared with donor-matched, first-trimester pEVTs and iEVTs at the level of global gene expression. Analyses of the latter revealed several biological processes involved in the transition from pEVT to iEVT. Besides IL-6-STAT3, TGF-β signaling, and
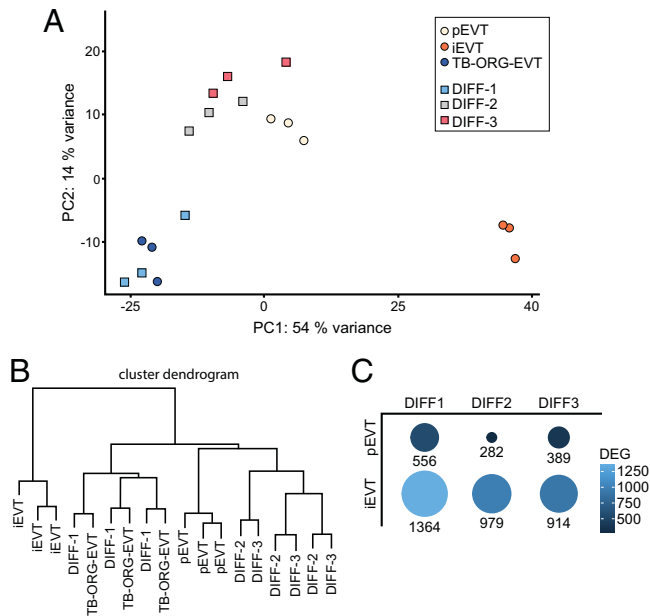
Fig. 6. Comparative gene expression analyses of HLA-G⁺ TB-ORG-EVTs (n = 3; derived from organoid cultures of sixth- to eighth-week placentae), isolated after cultivation in medium DIFF-1 (WNT⁻ A8301⁺), DIFF-2 (WNT⁻ A8301⁻), or DIFF-3 (WNT⁻ A8301⁻/TGF-β1⁺), and the donor-matched EVT samples analyzed in Fig. 2. (A) PCA showing clustering of pEVTs, iEVTs, and the in vitro EVTs, generated in the absence (TB-ORG-EVTs and DIFF-1) or presence (DIFF-2 and DIFF-3) of TGF-β signaling. Please note that TB-ORG-EVTs and DIFF-1 samples represent identical conditions, derived from two different sets of experiments. (B) Dendrogram depicting hierarchical clustering of the different EVT samples. (C) Correlation dot plot depicting the number of differentially expressed genes (DEGs) between pEVT and DIFF-1/DIFF-2/DIFF-3. Differential expression was defined based on an adjusted P value below 0.05 and an absolute log2 fold change above 1.5.

others, iEVTs displayed enrichment of a gene set characteristic for angiogenesis (*SI Appendix,* Fig. S3*A*). For instance, iEVTs expressed elevated transcript levels of secreted angiogenic proteins such as *FLT1, ISM2, ADM,* and *GRN* (*SI Appendix,* Fig. S2*F*). Expression of these factors could be associated with EVT-dependent spiral artery remodeling resembling angiogenesis at its initial stages (58). TGF-β, a known regulator of vascular remodeling (59), could be critically involved since transcript levels of some of the above-mentioned factors were increased upon TGF-β activation (*SI Appendix,* Fig. S7).

The only genes significantly down-regulated in iEVTs vs. pEVTs were targets of MYC (*SI Appendix,* Fig. S3*A*). This could be indicative of the decreasing mitotic activity during EVT differentiation. However, MYC has also been implicated in the acquisition of polyploidy and its placental expression is predominantly detected in the CC, where pEVTs undergo genome amplification (27, 28, 60). This process could be mitigated in decidual iEVTs. It is noteworthy that WNT-β-catenin signaling also showed a trend to decrease during iEVT formation (*SI Appendix,* Fig. S3*A*), coinciding with the reduced mRNA expression of *TCFL2*/TCF-4 in iEVTs (*SI Appendix,* Fig. S2*B*) and differentiated TB-ORGs (*SI Appendix,* Fig. S7). TCF-4, which is also a WNT target gene, controls expression of EVT markers such as ITGA5 and NOTCH2 (32). Transcript levels of these genes were lower in iEVTs compared with pEVTs (*SI Appendix,* Fig. S2*B*). Down-regulation of WNT signaling could be explained by the paracrine effects of the soluble WNT inhibitor DKK1, abundantly expressed by decidual stromal cells (42), providing a mechanism to limit the depth of trophoblast invasion (61). In addition, high concentrations of *NOTUM* (*SI Appendix,* Fig. S2*F*), a serine hydrolase inactivating secreted WNT ligands (62), as well as the diminished expression of components of the heterodimeric WNT receptors (*FZD5, FZD6, LRP5, LRP6*) in iEVTs and TGF-β–activated TB-ORG-EVTs (*SI Appendix,* Fig. S7) could promote autocrine down-regulation of the pathway.

Modest changes in biological processes were observed between patient-matched pEVTs and TB-ORG-EVTs, although each of the two EVT populations expressed unique genes (Fig. 2*B* and *SI Appendix,* Fig. S3*B*). Indeed, TB-ORG-EVTs developed in an artificial 3D environment which might have affected EVT maturation. In this regard, it is worth mentioning that A8301-treated TB-ORG-EVTs and villous explant cultures expressed higher levels of *CDH5*/VE-cadherin (e.g., Figs. 3*B* and 4*B*). VE-cadherin is a critical component of endothelial adherens junctions and has been identified as a marker of the adhesion phenotype of eEVTs (24). However, VE-cadherin is also specifically expressed in an intermediate region of the CC in TB-ORGs (*SI Appendix,* Fig. S2*E*) and placental tissues (27). The absence of TGF-β signaling in TB-ORG-EVTs/DIFF-1 could provoke accumulation of less-matured EVTs. Indeed, VE-cadherin⁺ pEVTs represent the first HLA-G⁺ cells that develop during EVT differentiation, whereas pEVTs of the distal CC and iEVTs lack VE-cadherin protein. Alternatively, TGF-β might switch off its expression in TB-ORGs (Fig. 3*B*). Indeed, TGF-β was shown to suppress VE-cadherin in trophoblastic HTR-8/SVneo cells, thereby decreasing invasion (63). However, its role might differ in pEVTs since down-regulation of VE-cadherin in the distal CC correlated with acquisition of the invasive phenotype.

Like in other epithelial cell types, TGF-β signaling could control trophoblast cell expansion. While recombinant TGF-β1 could increase villous CTB proliferation, possibly through ERK activation and linker-phosphorylated SMAD2, it was shown to impair proliferation of immortalized trophoblasts (64–66).

Since outgrowth in villous explant cultures occurred in the absence or presence of A8301 (Fig. 4), TGF-β signaling may have little effect on CC proliferation. However, our results suggest that TGF-β impaired EVT motility since A8301 provoked formation of stress fibers as well as focal adhesions at the leading edge of primary EVTs and increased their migratory capacity (Fig. 5 and *SI Appendix,* Fig. S6). These data are in line with different reports showing down-regulation of invasion of primary trophoblast and trophoblastic cell lines in the presence of recombinant TGF-β ligands (57). Since iEVTs expressed elevated levels of *TIMP*s and *SERPINE*s (*SI Appendix,* Fig. S2 *C and F*), invasion, mediated through MMPs and uPA (67, 68), could be further attenuated when cells reach deeper regions of the decidua.

TGF-β is likely to perform multiple tasks during EVT development. Whereas levels of *TGFBR1* and *TGFBR2* were low in pEVTs and TB-ORG-EVTs (DIFF-1), SMAD3 was induced in TB-ORG-EVTs that developed in the absence of WNT and TGF-β signaling (Fig. 4*C* and *SI Appendix,* Fig. S3*F*). However, nuclear recruitment of SMAD3 only occurred in a subset of the outermost pEVTs of the distal CC in vivo as well as in migratory TB-ORG-EVTs when A8301 was removed and recombinant TGF-β was added (Fig. 4*D* and *SI Appendix,* Fig. S4*H*). Accordingly, canonical activation of SMAD3 by C-terminal phosphorylation (pSMAD3C) was detected in TGF-β–treated TB-ORG-EVTs and differentiating primary EVTs, the latter activating the pathway in an autocrine manner (Fig. 4*E* and *SI Appendix,* Fig. S4*J*). In vivo, pSMAD3C was observed in the outer areas of distal CCs and conditioned medium of isolated decidual stromal cells was shown to increase SMAD3 phosphorylation in primary EVTs (66). In summary, we speculate that TGF-β, present in the adjacent decidua and in the Matrigel surrounding TB-ORG-EVTs, promotes nuclear recruitment and phosphorylation of SMAD3 (69). Together with SMAD4 and pSMAD2C, expressed in nuclei of pEVTs (66), functional SMAD transcription factors could be formed. In summary, pSMAD2C/3C in the outer pEVTs of the distal CC suggested active TGF-β signaling in these cells. Accordingly, activation of TGF-β signaling in TB-ORG-EVTs increased the similarity to pEVTs at the level of global gene expression (Fig. 6).

TGF-β–controlled differentiation may not only recapitulate features of pEVTs but also aspects of iEVTs since autocrine activation of the pathway (DIFF-2) reduced the number of differentially expressed genes between iEVTs and TB-ORG-EVTs (DIFF-1). However, TGF-β signaling can only partly stimulate differentiation into iEVTs, the latter forming a distinct cluster in the PCA (Fig. 6). Indeed, numerous growth factor and signaling cascades have been discovered in EVTs that may further shape gene expression and function of iEVTs (25, 50).

Nevertheless, TGF-β-SMAD3 could play an important role in the differentiation of pEVTs into iEVTs. The latter showed abundant nuclear SMAD3, as well as up-regulation of TGFβR1 and TGFβR2 (*SI Appendix,* Figs. S3 *F and G and S4H*). Elevated levels of TGF-β receptors could be critical for the paracrine activation of SMAD3, mediated through TGF-β ligands secreted from the decidua (57). Enhanced TGF-β signaling in iEVTs might be crucial for developing their secretory phenotype. Besides the aforementioned angiogenic factors and regulator of invasion, TGF-β signaling controlled PAPPA2 and DAO, two enzymes that are expressed by the majority of decidual iEVTs (Fig. 2*D*). Investigations in different trophoblast models suggested that TGF-β-ALK5 promoted expression and secretion of PAPPA2 and DAO and provoked recruitment of SMAD3 to the promoter/enhancer regions of their genes. Accordingly, siRNA-mediated
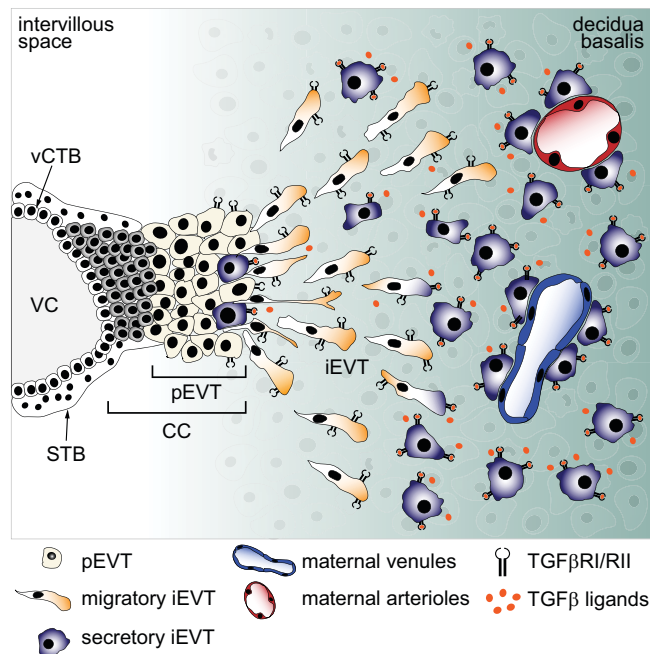
Fig. 7. Schematic depiction of the developmental process of EVTs. Activation of TGF-β signaling differentiates migratory iEVTs into secretory iEVTs with reduced migratory capacity.

silencing of *TGFBR1*, *TGFBR2*, and *SMAD3* in primary EVTs and differentiating TSCs as well as chemical inhibition of SMAD3 in TGF-β–activated TB-ORG-EVTs down-regulated expression of these iEVT markers (Fig. 4 *F–J* and *SI Appendix,* Fig. S4 *L–O*). PAPPA2 likely regulates trophoblast motility, since it cleaves specific IGFBPs which control the bioavailability of promigratory IGFs (70). However, DAO is a histamine-degrading enzyme that within the placenta is exclusively expressed and secreted by EVTs (33). Its expression in decidual iEVTs was shown to increase when the cells approach decidual arterial and venous vessels. Indeed, DAO was already detected at the seventh week of gestation in the serum of pregnant women and showed significantly lower levels in early-onset preeclampsia (33). Hence, TGF-β could be critical for the secretion of iEVT-specific products into the decidual veins, thereby modulating metabolic functions of the mother, at a time when spiral arteries are still thought to be plugged (9).

In summary, the present data suggest that TGF-β signaling plays a pivotal role in extravillous differentiation (Fig. 7). Removal of WNT activation allows for formation of CCs and HLA-G⁺ EVTs, whereas activation of TGF-β signaling in pEVTs, contacting the maternal decidua, could be required for EVT maturation. It is noteworthy that only a small subset of pEVTs, expressing DAO and PAPPA2, undergoes differentiation into an iEVT phenotype in the distal CC (Fig. 4A). Hence, we speculate that in the majority of distal pEVTs, TGF-β-SMAD3 signaling is not fully activated, allowing for detachment and migration into the maternal environment. In the decidua, iEVTs up-regulate TGF-β

receptors and TGF-β signaling, thereby slowing down migration and promoting differentiation into a secretory iEVT phenotype. However, TGF-β only partly accounts for the features of iEVTs, since the present RNA-seq data also suggest considerable differences between iEVTs and the TGF-β–activated TB-ORG-EVTs (Fig. 6C). Additional analyses of critical signaling pathways and their temporal activation are needed to further optimize in vitro formation and differentiation of EVTs. Moreover, single-cell RNA-seq analyses will further unravel the heterogeneity of the different in vivo EVT populations.

Materials and Methods

Tissue Collection. First-trimester placental and decidual tissue (sixth to eighth week of gestation, n = 51) was obtained from legal pregnancy terminations. Utilization of tissues and all experimental procedures were approved by the ethics boards of the Medical University of Vienna (no. 084/2009), and required written informed consent from donating women. For isolation of patient-matched pEVTs and iEVTs, placenta and decidua basalis were collected from the same single donor. Unless stated otherwise, all cell isolations were performed from single placentae.

EVT Differentiation in TB-ORGs. For TGF-β experiments, TB-ORGs at passage 2 were split into 48 domes supplemented with 50 ng/mL EGF, with/without 2 μM A8301, and with/without 5 ng/mL recombinant TGF-β1 (Abcam). After evaluation of these conditions (*SI Appendix*, Fig. S4 *A and B*), the following protocol was finally applied: An initial differentiation mixture (bTOM containing 50 ng/mL rhEGF and 2 μM A8301) was added to the cultures for 5 d. Afterward, the TB-ORG domes were washed and prewarmed bTOM was added for 1 h at 37 °C. Subsequently, three different media were supplemented for another 5 d: bTOM containing 2 μM A8301 and 50 ng/mL EGF (DIFF-1), bTOM containing 50 ng/mL rhEGF (DIFF-2), and bTOM containing 50 ng/mL EGF and 5 ng/mL TGF-β1 (DIFF-3). For SMAD3 inhibition during differentiation, 10 μM SMAD3 inhibitor SIS3 (Calbiochem) was supplemented from day 6 to 10. During differentiation, culture media were changed every 2 to 3 d. At the end of the experiments, a fraction of TB-ORG domes was fixed for paraffin embedding and subsequent immunofluorescence analyses. For RNA and protein isolation, TB-ORG-EVTs were purified using HLA-G-PE antibodies and anti-PE MicroBeads, respectively, as described in *SI Appendix, Methods*.

For an additional description of methods, see *SI Appendix, Methods*.

Data Availability. The RNA-seq data reported in this article have been deposited in the GEO (accession no. GSE188352) (71).

All study data are included in the article and/or supporting information.

Author affiliations: ᵃPlacental Development Group, Reproductive Biology Unit, Department of Obstetrics and Gynaecology, Medical University of Vienna, Vienna, 1090 Austria; ᵇFetal-Maternal Immunology Group, Reproductive Biology Unit, Department of Obstetrics and Gynaecology, Medical University of Vienna, Vienna, 1090 Austria; ᶜGynmed Clinic, 1150 Vienna, Austria; and ᵈCenter for Anatomy and Cell Biology, Medical University of Vienna, 1090 Vienna, Austria

1. A. Erlebacher, Immunology of the maternal-fetal interface. *Annu. Rev. Immunol.* **31**, 387–411 (2013).
2. D. Evain-Brion, A. Malassine, Human placenta as an endocrine organ. *Growth Horm. IGF Res.* **13**, S34–S37 (2003).
3. T. Napso, H. E. J. Yong, J. Lopez-Tello, A. N. Sferruzzi-Perri, The role of placental hormones in mediating maternal adaptations to support pregnancy and lactation. *Front. Physiol.* **9**, 1091 (2018).
4. W. J. Hamilton, J. D. Boyd, Development of the human placenta in the first three months of gestation. *J. Anat.* **94**, 297–328 (1960).
5. G. J. Burton, A. L. Fowden, The placenta: A multifaceted, transient organ. *Philos. Trans. R. Soc. Lond. B Biol. Sci.* **370**, 20140066 (2015).

6. R. Pijnenborg, J. M. Bland, W. B. Robertson, I. Brosens, Uteroplacental arterial changes related to interstitial trophoblast migration in early human pregnancy. *Placenta* **4**, 397–413 (1983).
7. R. Pijnenborg, G. Dixon, W. B. Robertson, I. Brosens, Trophoblastic invasion of human decidua from 8 to 18 weeks of pregnancy. *Placenta* **1**, 3–19 (1980).
8. K. M. Varberg, M. J. Soares, Paradigms for investigating invasive trophoblast cell development and contributions to uterine spiral artery remodeling. *Placenta* **113**, 48–56 (2021).
9. G. J. Burton, E. Jauniaux, D. S. Charnock-Jones, The influence of the intrauterine environment on human placental development. *Int. J. Dev. Biol.* **54**, 303–312 (2010).
10. S. D. Smith, C. E. Dunk, J. D. Aplin, L. K. Harris, R. L. Jones, Evidence for immune cell involvement in decidual spiral arteriole remodeling in early human pregnancy. *Am. J. Pathol.* **174**, 1959–1971 (2009).

11. R. Pijnenborg, L. Vercruysse, M. Hanssens, The uterine spiral arteries in human pregnancy: Facts and controversies. *Placenta* **27**, 939–958 (2006).

12. C. H. Damsky, M. L. Fitzgerald, S. J. Fisher, Distribution patterns of extracellular matrix components and adhesion receptors are intricately modulated during first trimester cytotrophoblast differentiation along the invasive pathway, in vivo. *J. Clin. Invest.* **89**, 210–222 (1992).

13. Y. Zhou *et al.*, Human cytotrophoblasts adopt a vascular phenotype as they differentiate. A strategy for successful endovascular invasion? *J. Clin. Invest.* **99**, 2139–2151 (1997).

14. G. J. Burton, A. L. Watson, J. Hempstock, J. N. Skepper, E. Jauniaux, Uterine glands provide histiotrophic nutrition for the human fetus during the first trimester of pregnancy. *J. Clin. Endocrinol. Metab.* **87**, 2954–2959 (2002).

15. G. Moser, K. Weiss, M. Gauster, M. Sundl, B. Huppertz, Evidence from the very beginning: Endoglandular trophoblasts penetrate and replace uterine glands in situ and in vitro. *Hum. Reprod.* **30**, 2747–2757 (2015).

16. G. Moser *et al.*, Extravillous trophoblasts invade more than uterine arteries: Evidence for the invasion of uterine veins. *Histochem. Cell Biol.* **147**, 353–366 (2017).

17. K. Windsperger *et al.*, Extravillous trophoblast invasion of venous as well as lymphatic vessels is altered in idiopathic, recurrent, spontaneous abortions. *Hum. Reprod.* **32**, 1208–1217 (2017).

18. T. Y. Khong, F. De Wolf, W. B. Robertson, I. Brosens, Inadequate maternal vascular response to placentation in pregnancies complicated by pre-eclampsia and by small-for-gestational age infants. *Br. J. Obstet. Gynaecol.* **93**, 1049–1059 (1986).

19. R. Pijnenborg *et al.*, Placental bed spiral arteries in the hypertensive disorders of pregnancy. *Br. J. Obstet. Gynaecol.* **98**, 648–655 (1991).

20. R. Romero, J. P. Kusanovic, T. Chaiworapongsa, S. S. Hassan, Placental bed disorders in preterm labor, preterm PROM, spontaneous abortion and abruptio placentae. *Best Pract. Res. Clin. Obstet. Gynaecol.* **25**, 313–327 (2011).

21. O. Farah, C. Nguyen, C. Tekkatte, M. M. Parast, Trophoblast lineage-specific differentiation and associated alterations in preeclampsia and fetal growth restriction. *Placenta* **102**, 4–9 (2020).

22. K. H. Lim *et al.*, Human cytotrophoblast differentiation/invasion is abnormal in pre-eclampsia. *Am. J. Pathol.* **151**, 1809–1818 (1997).

23. R. W. Redline, P. Patterson, Pre-eclampsia is associated with an excess of proliferative immature intermediate trophoblast. *Hum. Pathol.* **26**, 594–600 (1995).

24. Y. Zhou, C. H. Damsky, S. J. Fisher, Preeclampsia is associated with failure of human cytotrophoblasts to mimic a vascular adhesion phenotype. One cause of defective endovascular invasion in this syndrome? *J. Clin. Invest.* **99**, 2152–2164 (1997).

25. J. Pollheimer, S. Vondra, J. Baltayeva, A. G. Beristain, M. Knöfler, Regulation of placental extravillous trophoblasts by the maternal uterine environment. *Front. Immunol.* **9**, 2597 (2018).

26. M. Knöfler *et al.*, Human placenta and trophoblast development: Key molecular mechanisms and model systems. *Cell. Mol. Life Sci.* **76**, 3479–3496 (2019).

27. S. Haider *et al.*, Notch1 controls development of the extravillous trophoblast lineage in the human placenta. *Proc. Natl. Acad. Sci. U.S.A.* **113**, E7710–E7719 (2016).

28. P. Velicky *et al.*, Genome amplification and cellular senescence are hallmarks of human placenta development. *PLoS Genet.* **14**, e1007698 (2018).

29. S. Kovats *et al.*, A class I antigen, HLA-G, expressed in human trophoblasts. *Science* **248**, 220–223 (1990).

30. K. Plessl, S. Haider, C. Fiala, J. Pollheimer, M. Knöfler, Expression pattern and function of Notch2 in different subtypes of first trimester cytotrophoblast. *Placenta* **36**, 365–371 (2015).

31. V. Fock *et al.*, Neuregulin-1-mediated ErbB2-ErbB3 signalling protects human trophoblasts against apoptosis to preserve differentiation. *J. Cell Sci.* **128**, 4306–4316 (2015).

32. G. Meinhardt *et al.*, Wnt-dependent T-cell factor-4 controls human etravillous trophoblast motility. *Endocrinology* **155**, 1908–1920 (2014).

33. P. Velicky *et al.*, Pregnancy-associated diamine oxidase originates from extravillous trophoblasts and is decreased in early-onset preeclampsia. *Sci. Rep.* **8**, 6342 (2018).

34. R. Vento-Tormo *et al.*, Single-cell reconstruction of the early maternal-fetal interface in humans. *Nature* **563**, 347–353 (2018).

35. S. Haider *et al.*, Self-renewing trophoblast organoids recapitulate the developmental program of the early human placenta. *Stem Cell Reports* **11**, 537–551 (2018).

36. H. Okae *et al.*, Derivation of human trophoblast stem cells. *Cell Stem Cell* **22**, 50–63.e6 (2018).

37. M. Y. Turco *et al.*, Trophoblast organoids as a model for maternal-fetal interactions during human placentation. *Nature* **564**, 263–267 (2018).

38. G. Meinhardt *et al.*, Pivotal role of the transcriptional co-activator YAP in trophoblast stemness of the developing human placenta. *Proc. Natl. Acad. Sci. U.S.A.* **117**, 13562–13570 (2020).

39. G. Gaus *et al.*, Extracellular pH modulates the secretion of fibronectin isoforms by human trophoblast. *Acta Histochem.* **104**, 51–63 (2002).

40. A. Samalecos *et al.*, Characterization of a novel telomerase-immortalized human endometrial stromal cell line, St-T1b. *Reprod. Biol. Endocrinol.* **7**, 76 (2009).

41. K. Imai *et al.*, Human endometrial stromal cells and decidual cells express cluster of differentiation (CD) 13 antigen/aminopeptidase N and CD10 antigen/neutral endopeptidase. *Biol. Reprod.* **46**, 328–334 (1992).

42. S. Tulac *et al.*, Dickkopf-1, an inhibitor of Wnt signaling, is regulated by progesterone in human endometrial stromal cells. *J. Clin. Endocrinol. Metab.* **91**, 1453–1461 (2006).

43. E. M. Rutanen, E. Gonzalez, J. Said, G. D. Braunstein, Immunohistochemical localization of the insulinlike growth factor binding protein-1 in female reproductive tissues by monoclonal antibodies. *Endocr. Pathol.* **2**, 132–138 (1991).

44. V. Fock *et al.*, Trophoblast subtype-specific EGFR/ERBB4 expression correlates with cell cycle progression and hyperplasia in complete hydatidiform moles. *Hum. Reprod.* **30**, 789–799 (2015).

45. B. Huppertz, S. Kertschanska, A. Y. Demir, H. G. Frank, P. Kaufmann, Immunohistochemistry of matrix metalloproteinases (MMP), their substrates, and their inhibitors (TIMP) during trophoblast invasion in the human placenta. *Cell Tissue Res.* **291**, 133–148 (1998).

46. S. Bauer *et al.*, Tumor necrosis factor-alpha inhibits trophoblast migration through elevation of plasminogen activator inhibitor-1 in first-trimester villous explant cultures. *J. Clin. Endocrinol. Metab.* **89**, 812–822 (2004).

47. J. Wang *et al.*, Expression of pregnancy-associated plasma protein A2 during pregnancy in human and mouse. *J. Endocrinol.* **202**, 337–345 (2009).

48. M. Jinnin, H. Ihn, K. Tamaki, Characterization of SIS3, a novel specific inhibitor of Smad3, and its effect on transforming growth factor-beta1-induced extracellular matrix expression. *Mol. Pharmacol.* **69**, 597–607 (2006).

49. L. M. McHardy, K. Warabi, R. J. Andersen, C. D. Roskelley, M. Roberge, Strongylophorine-26, a Rho-dependent inhibitor of tumor cell invasion that reduces actin stress fibers and induces nonpolarized lamellipodial extensions. *Mol. Cancer Ther.* **4**, 772–778 (2005).

50. M. Knöfler, Critical growth factors and signalling pathways controlling human trophoblast invasion. *Int. J. Dev. Biol.* **54**, 269–280 (2010).

51. C. Q. E. Lee *et al.*, Integrin $\alpha 2$ marks a niche of trophoblast progenitor cells in first trimester human placenta. *Development* **145**, dev162305 (2018).

52. A. K. Wakeland *et al.*, Hypoxia directs human extravillous trophoblast differentiation in a hypoxia-inducible factor-dependent manner. *Am. J. Pathol.* **187**, 767–780 (2017).

53. K. M. Varberg *et al.*, ASCL2 reciprocally controls key trophoblast lineage decisions during hemochorial placenta development. *Proc. Natl. Acad. Sci. U.S.A.* **118**, e2016517118 (2021).

54. G. Castel *et al.*, Induction of human trophoblast stem cells from somatic cells and pluripotent stem cells. *Cell Rep.* **33**, 108419 (2020).

55. S. Io *et al.*, Capturing human trophoblast development with naive pluripotent stem cells in vitro. *Cell Stem Cell* **28**, 1023–1039.e13 (2021).

56. R. L. Jones, C. Stoikos, J. K. Findlay, L. A. Salamonsen, TGF-beta superfamily expression and actions in the endometrium and placenta. *Reproduction* **132**, 217–232 (2006).

57. Y. Li, J. Yan, H. M. Chang, Z. J. Chen, P. C. K. Leung, Roles of TGF-β superfamily proteins in extravillous trophoblast invasion. *Trends Endocrinol. Metab.* **32**, 170–189 (2021).

58. J. H. Distler *et al.*, Angiogenic and angiostatic factors in the molecular control of angiogenesis. *Q. J. Nucl. Med.* **47**, 149–161 (2003).

59. M. J. Goumans, Z. Liu, P. ten Dijke, TGF-beta signaling in vascular biology and dysfunction. *Cell Res.* **19**, 116–127 (2009).

60. M. J. Muñoz-Alonso *et al.*, MYC accelerates p21CIP-induced megakaryocytic differentiation involving early mitosis arrest in leukemia cells. *J. Cell. Physiol.* **227**, 2069–2078 (2012).

61. J. Pollheimer *et al.*, Activation of the canonical Wingless/T-cell factor signaling pathway promotes invasive differentiation of human trophoblast. *Am. J. Pathol.* **168**, 1134–1147 (2006).

62. V. I. Torres, J. A. Godoy, N. C. Inestrosa, Modulating Wnt signaling at the root: Porcupine and Wnt acylation. *Pharmacol. Ther.* **198**, 34–45 (2019).

63. J. C. Cheng, H. M. Chang, P. C. Leung, Transforming growth factor-β1 inhibits trophoblast cell invasion by inducing Snail-mediated down-regulation of vascular endothelial-cadherin protein. *J. Biol. Chem.* **288**, 33181–33192 (2013).

64. K. Forbes, B. Souquet, R. Garside, J. D. Aplin, M. Westwood, Transforming growth factor-beta (TGFbeta) receptors I/II differentially regulate TGFbeta1 and IGF-binding protein-3 mitogenic effects in the human placenta. *Endocrinology* **151**, 1723–1731 (2010).

65. C. H. Graham, J. J. Lysiak, K. R. McCrae, P. K. Lala, Localization of transforming growth factor-beta at the human fetal-maternal interface: Role in trophoblast growth and differentiation. *Biol. Reprod.* **46**, 561–572 (1992).

66. S. Haider, V. Kunihs, C. Fiala, J. Pollheimer, M. Knöfler, Expression pattern and phosphorylation status of Smad2/3 in different subtypes of human first trimester trophoblast. *Placenta* **57**, 17–25 (2017).

67. P. Bischoff, A. Meisser, A. Campana, Paracrine and autocrine regulators of trophoblast invasion–A review. *Placenta* **21**, S55–S60 (2000).

68. P. K. Lala, C. Chakraborty, Factors regulating trophoblast migration and invasiveness: Possible derangements contributing to pre-eclampsia and fetal injury. *Placenta* **24**, 575–587 (2003).

69. J. Massagué, TGFβ signalling in context. *Nat. Rev. Mol. Cell Biol.* **13**, 616–630 (2012).

70. J. K. Christians, A. G. Beristain, ADAM12 and PAPP-A: Candidate regulators of trophoblast invasion and first trimester markers of healthy trophoblasts. *Cell Adhes. Migr.* **10**, 147–153 (2016).

71. S. Haider, Martin Knöfler, A. Ian Lackner, Next generation sequencing of human first trimester placental EVTs (pEVT), decidual interstitial EVTs (iEVT), and trophoblast organoid (TB-ORG)-derived extravillous trophoblasts (TB-ORG-EVTs). GEO Data Base. https://www.ncbi.nlm.nih.gov/geo/query/acc.cgi?acc=GSE188352. Deposited 6 November 2021.